Progress In Electromagnetics Research M, Vol. 62, 189–198, 2017

A 2 to 4 GHz Instantaneous Frequency Measurement System Using Multiple Band-Pass Filters

Hossam Badran* **and Mohammad Deeb**

Abstract—In this paper, a 2 to 4 GHz Instantaneous Frequency Measurement (IFM) system is presented. The proposed design uses four band-pass filters to estimate the frequency value of an RF signal. The proposed design is an improvement of that presented in our previously published work. In this work, a new frequency estimator is developed, and a new methodology for designing the frequency response of the band-pass filters is proposed. These two improvements show better accuracy in estimating the frequency value. A closed form for the Standard Deviation (STD) and the bias of the new estimator were derived, and used to adjust the frequency response of the filters. The fabricated system showed a maximum error of about 11 MHz, for practical values of noise and measurements errors.

1. INTRODUCTION

Determining the carrier frequency of the received RF signal is an essential mission performed by many Electronic Warfare (EW) systems. Most EW systems use Instantaneous Frequency Measurement (IFM) sub-systems to perform this job [1, 2]. A conventional IFM, measures the phase between the received signal and a delayed version of it to extract the frequency information. A delay line is used to generate the delayed signal, and a phase discriminator to measure the phase difference [3, 4]. A phase discriminator is often implemented using power dividers, hybrid couplers, and square law detectors [5].

To obtain high accuracy in measuring the frequency, the elements of the IFM system must be carefully designed, fabricated, and integrated. Very good matching and isolation between the components, high sensitivity of the detectors, good stability of the delay line versus temperature changes, and the compensation of the delay line loss by an equal loss in the direct path are needed [1, 6]. To respond to these requirements, high fabrication technology must be used which increases the cost.

In our previously published work [7], we proposed a simple low cost method for implementing an IFM system and presented a design example with working frequency band of 2 to 4 GHz. The presented design showed a maximum error of about 15 MHz. In this paper an improved accuracy IFM system is presented. The new design uses a new method for estimating the frequency value, and a new methodology for designing the frequency response of the filters.

2. DESCRIPTION OF THE PROPOSED DESIGN

The block diagram of the proposed IFM system is shown in Figure 1. At the input of the system, a limiting amplifier is placed followed by a 4-way power divider. At each output port of the power divider a band-pass filter is connected, followed by a logarithmic detector and an analog to digital convertor (ADC). Each filter with the corresponding logarithmic detector and the ADC form a so called channel.

Received 16 October 2017, Accepted 15 November 2017, Scheduled 29 November 2017

* Corresponding author: Hossam Badran (hossam.m.badran@gmail.com).
The authors are with the Department of communication engineering, Higher Institute for Applied Science and technology, Damascus, Syria.

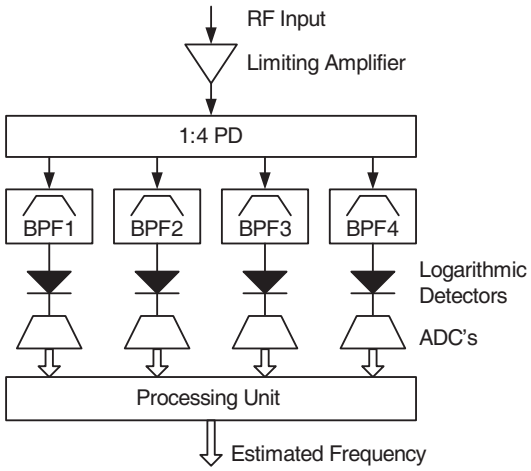

Figure 1. Block diagram of the proposed IFM system.

The digital data from the four ADC's are fed to a processing unit which will calculate an estimation of the frequency value.

Although the block diagram of the system is the same as the one used in the previous work, this design differs from the previous work by the frequency response of the filters. Figure 2(a) shows the frequency responses of the filters used in the previous design, while Figure 2(b) shows the frequency responses of the filters used in this design.

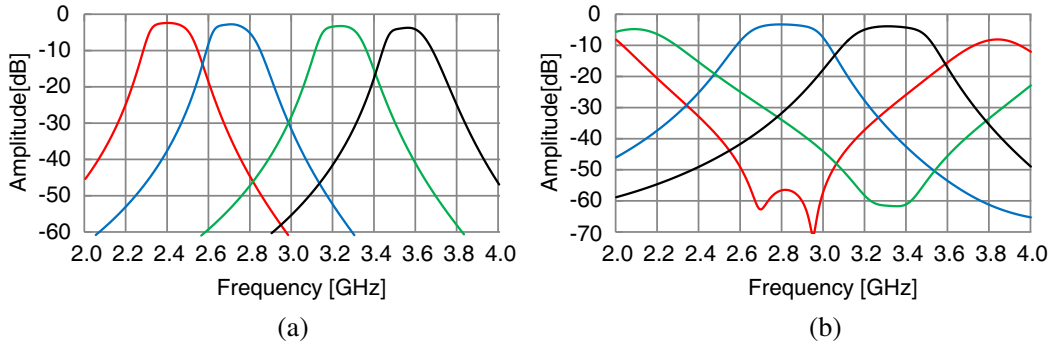

Figure 2. Frequency response of BPF1 (red), BPF2 (blue), BPF3 (green), and BPF4 (black). For: (a) the previous IFM system, (b) the current IFM system.

It is seen that the frequency responses of the new filters overlap each other, so that at each frequency point, there exists a frequency response with a significant positive slope, and another frequency response with a significant negative slope. This design gives an advantage to the new method in estimating the frequency described in Section 4. The new frequency estimation method gives better accuracy by minimizing the bias of the estimator.

Note that more filters can be used to increase the system accuracy, but this will increase the complexity of the system. In this design we use four filters to minimize the system complexity.

An RF signal present at the system input will be amplified by the limiting amplifier to a known power level P_{sat}, then it will be divided by a 4-way power divider into four signals with equal amplitudes. Each signal will pass through one of the band-pass filters, where it will be attenuated according to its frequency by the corresponding filter. The powers of the filtered signals are measured by the logarithmic detectors and digitized by the ADCs. The acquired data are then fed to the processing unit, which will calculate an estimation for the frequency value.

In this work, the used limiting amplifier has a nominal output power level of $P_{\text{sat}} = 0\,\text{dBm}$. And

the AD8318 logarithmic detector from ANALOG DEVICES is used to measure the power level of the filtered signals. The logarithmic detector produces a voltage proportional to the power level of the signal at its input expressed in dBm, given by:

$$Vo = m(P_{\text{in}} - P_{\text{intercept}}) \tag{1}$$

where P_{in} is the input signal power level expressed in dBm, m the slope of the detector's transfer function expressed in Volt/dB, and $P_{\text{intercept}}$ the intercept point expressed in dBm. The value of the slope m and $P_{\text{intercept}}$ vary slightly with frequency.

Equation (1) is valid only if the power of the input signal is within the detector dynamic interval $P_{\text{det-min}}$ to $P_{\text{det-max}}$.

The characteristics of the AD8318 are stated over the frequency band 1.9 to 5.8 GHz as: the slope $m = -24.4\,\text{mV/dB}$, $P_{\text{intercept}}$ is from 19.6 to 25 dBm, and the dynamic interval is from -60 to -5 dBm.

3. THE MICROWAVE CIRCUIT OF THE SYSTEM

The microwave circuit of the system, which is the 4-way power divider and the four band-pass filters, was implemented on an FR-4(DE104) substrate using printed circuit board technology. The substrate has a dielectric constant of 4.2, loss tangent of 0.02, and thickness of 0.8 mm. The layout of this microwave circuit is shown in Figure 3(a), and a photo of it, with the limiting amplifier and the logarithmic detectors, is shown in Figure 3(b). The microwave circuit has one input port P1 and four output ports P2, P3, P4, and P5.

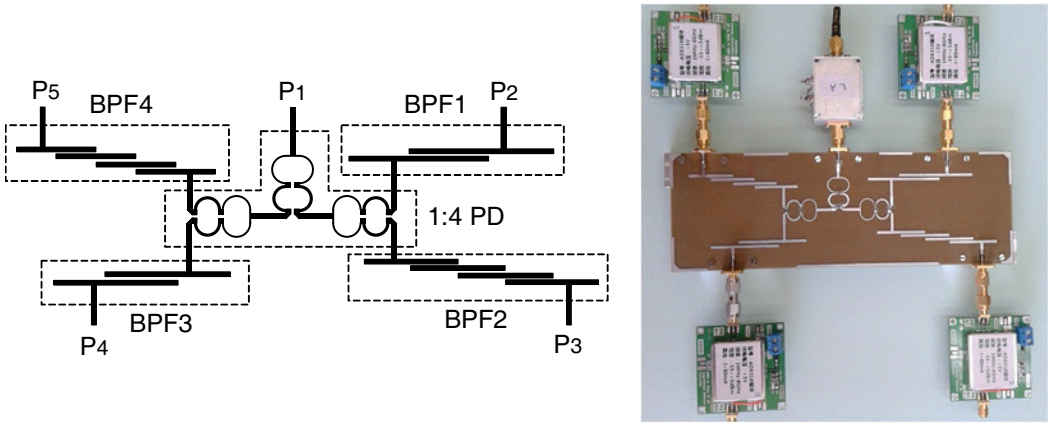

(a) (b)

Figure 3. (a) Layout of the microwave circuit, (b) a photo of the IFM system.

The 4-way power divider was implemented using three identical 2-way dividers, and each one is a two-section Wilkinson power divider designed at a center frequency of 3 GHz and bandwidth of 2 GHz. The most important characteristic of the divider is the isolation coefficient between its ports, and high isolation is needed to prevent interactions between the filters. The layout of the fabricated divider with physical dimensions is shown in Figure 4. The physical dimensions are shown in Table 1 (in mm). The used resistors are: $R_1 = 100\,\Omega$, and $R_2 = 300\,\Omega$.

The band-pass filters, BPF1 and BPF3, are second order coupled lines Butterworth filters with tapped input and output. They have the same topology that is shown in Figure 5(a).

The band-pass filters BPF2 and BPF4 are fourth order coupled lines Butterworth filters with tapped input and output. They have the same topology that is shown in Figure 5(b). The physical dimensions of these four filters are shown in Table 2 (in mm).

The transmission coefficients of the microwave circuit, $|S_{21}|$, $|S_{31}|$, $|S_{41}|$, and $|S_{51}|$, were calculated using the Advanced Design System software (ADS) (see Figure 6). It is shown that the frequency response at the circuit output ports has nearly the same shape of the filters frequency response when

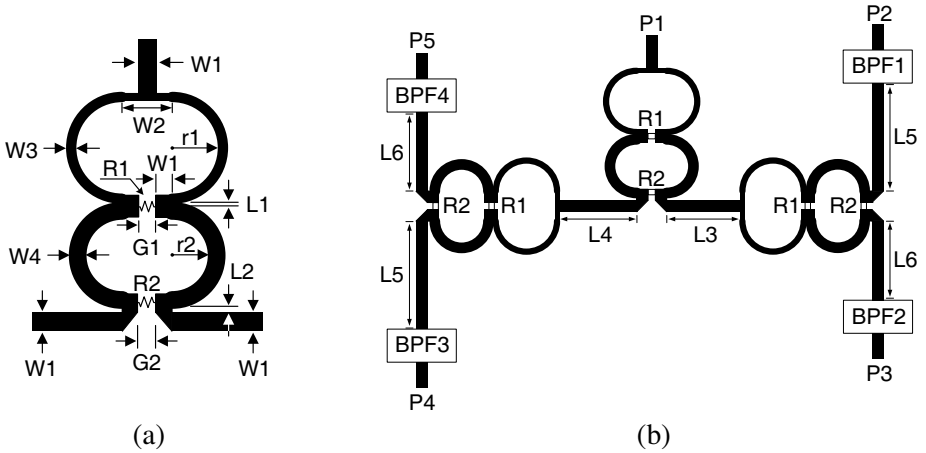

Figure 4. (a) Layout of the 2-way power divider, (b) layout of the 4-way power divider.

Table 1. Physical dimensions of the fabricated 4-way power divider (in mm).

Dimension		Dimension		Dimension	
W_1	1.58	r_2	3.72	L_3	10.22
W_2	4.16	G_1	1	L_4	10.76
W_3	0.61	G_2	1	L_5	15
W_4	1.06	L_1	0.2	L_6	11
r_1	4.25	L_2	0.5		

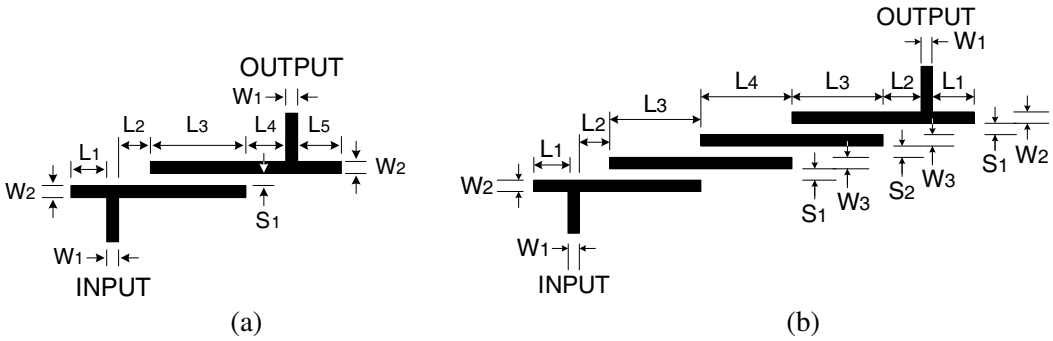

Figure 5. (a) Topology of BPF1 and BPF3, (b) topology of BPF2 and BPF4.

being measured separately, which is guaranteed by the high isolation between the output ports of the 4-way power divider.

After integrating the limiting amplifier and the logarithmic detectors with the microwave circuit, the transfer functions of the system must be measured. The transfer functions are the voltages at the output of the logarithmic detectors as a function of the incoming signal frequency. Each transfer function corresponds to one channel of the system. Measuring the transfer functions is done at a laboratory by applying a reference signal with known frequency f_m at the system input, and measuring the voltages at the logarithmic detectors outputs, then the frequency f_m is changed by small steps of 2 MHz to scan the working frequency band of the system 2 to 4 GHz. The measured voltages are stored into the four vectors G_1, G_2, G_3, and G_4 which will be the four transfer functions of the system.

Measuring the transfer functions by this way has an advantage that the non-ideal behaviour of the

Table 2. Physical dimensions of the designed filters (in mm).

	BPF1	BPF2	BPF3	BPF4
W_1	1.58	1.58	1.58	1.58
W_2	1.53	1.59	1.53	1.59
W_3	-	1.53	-	1.55
L_1	13.39	8.5	12.07	7.44
L_2	3.94	4.25	2.51	3.32

	BPF1	BPF2	BPF3	BPF4
L_3	24.73	14.88	22.97	12.51
L_4	3.94	14.76	2.59	12.43
L_5	14.77	-	11.67	-
S_1	0.87	0.48	1.11	0.6
S_2	-	0.83	-	0.99

system components is included in the measured transfer functions, such as: the variation of the nominal output power of the limiting amplifier P_{sat} with frequency, the amplitude imbalance at the divider output ports, and the variation of the logarithmic detector characteristic (the slope m, and $P_{\text{intercept}}$) with frequency.

The measured transfer functions of the fabricated system are shown in Figure 7. The transfer functions are clipped manually to a maximum value of 2 V. It is seen that the transfer functions have nearly the same shape of the filters frequency responses but with up down flipping. The differences between the filters frequency response and the transfer functions is due to the variation of the detectors characteristic with frequency, and the non-perfect matching of the components.

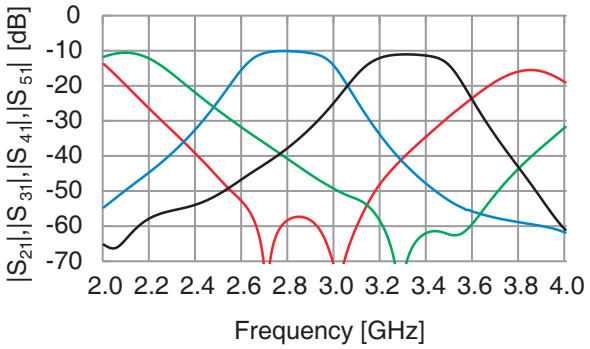

Figure 6. EM simulated transmission coefficients of the microwave circuit, $|S_{21}|$ with red, $|S_{31}|$ with blue, $|S_{41}|$ with green, and $|S_{51}|$ with black.

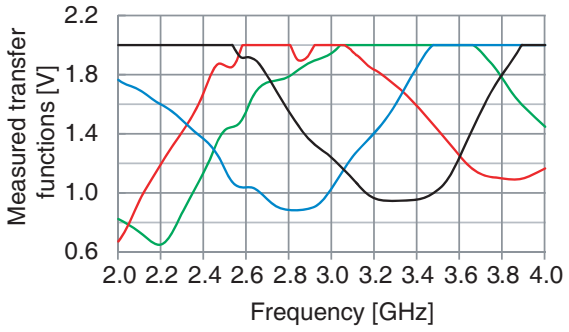

Figure 7. The measured transfer functions of the fabricated IFM system. G_1 with red, G_2 with blue, G_3 with green, and G_4 with black.

4. DATA MODEL AND FREQUENCY ESTIMATION

Consider that an RF signal with unknown frequency f_0 is present at the system input. The output voltages of the logarithmic detectors in channel number k can be written using the measured transfer functions G_k as:

$$V_{ok} = G_k(f_0) + n_k, \quad k = 1, \ldots, 4 \tag{2}$$

Here n_1, n_2, n_3, n_4 are the noise voltages at the detectors output and are assumed uncorrelated with zero mean and a variance of σ^2.

The output power level P_{sat} of the limiting amplifier may drift slightly from its nominal value due to temperature changes. This drift will be distributed equally between the four system's channels and appears as a voltage drift, named e_0, at the output of the four detectors.

Also, temperature changes make the output voltages of the detectors drifted from their nominal values, and these drifts are named e_1, e_2, e_3, e_4. Taking these voltage drifts into account, Equation (2) becomes:

$$V_{ok} = G_k(f_0) + e_0 + e_k + n_k, \quad k = 1, \ldots, 4 \tag{3}$$

The voltages $V_{o1}, \ldots, V_{o4}$ are sampled by the four ADCs. In practice, the samples are acquired during a short time interval, e.g., for pulsed RF signals, the sampling is performed only during the pulse width. Because the voltage drifts $e_0, \ldots, e_4$ are generated due to temperature changes, they have a slow variation nature and can be considered fixed during the time of acquiring samples. Consequently, the voltages $V_{o1}, \ldots, V_{o4}$ will be sampled as:

$$\begin{aligned} Z_1[i] &= G_1(f_0) + e_0 + e_1 + n_1[i] \\ Z_2[i] &= G_2(f_0) + e_0 + e_2 + n_2[i] \\ Z_3[i] &= G_3(f_0) + e_0 + e_3 + n_3[i] \\ Z_4[i] &= G_4(f_0) + e_0 + e_4 + n_4[i], \quad i = 1, \ldots, N \end{aligned} \tag{4}$$

Here N is the number of acquired samples.

These samples are fed to the processing unit, where the frequency value is estimated. In our previous work [7], the Least Square (LS) estimator was used, where the estimated value $\hat{f}_{0-\mathrm{LS}}$ of f_0 is the value that minimizes the function $J(f)$ in (5)

$$\begin{aligned} J(f) &= \sum_{i=1}^{N} \left[(Z_1[i] - G_1(f))^2 + (Z_2[i] - G_2(f))^2 + (Z_3[i] - G_3(f))^2 + (Z_4[i] - G_4(f))^2 \right] \\ \hat{f}_{0-\mathrm{LS}} &= \min_f \left(J(f) \right) \end{aligned} \tag{5}$$

It is shown that the LS estimator has a variance and a maximum absolute bias, given by Eqs. (6) and (7) respectively.

$$\mathrm{var}(\hat{f}_{0-\mathrm{LS}}) \approx \frac{\sigma^2/N}{A} \tag{6}$$

$$\begin{aligned} \max\_\mathrm{bias}(\hat{f}_{0-\mathrm{LS}}) \approx \frac{e_{\max}}{A} &\left[\left|G_1'(f_0)\right| + \left|G_2'(f_0)\right| + \left|G_3'(f_0)\right| + \left|G_4'(f_0)\right| \right. \\ &\left. + \left|G_1'(f_0) + G_2'(f_0) + G_3'(f_0) + G_{41}'(f_0)\right| \right] \end{aligned} \tag{7}$$

where

$$A = G_1'^2(f_0) + G_2'^2(f_0) + G_3'^2(f_0) + G_4'^2(f_0) \tag{8}$$

Here $e_{\max}$ is the maximum value of the voltage drifts e_0, e_1, e_2, e_3, e_4.

In this work, the LS estimator will be applied but with a different way. Examining Equations (4) shows that the voltage drift e_0 is present in all acquired data Z's and can be eliminated by subtracting the acquired samples from each other. Also examining Equation (7) shows that the maximum bias of the LS estimator is inversely proportional to the slope of the transfer functions, thus a transfer function G_k with higher slope has a lower contribution to the estimator's bias.

These two notes lead to proposing a new method for estimating the frequency. In this method, only the two transfer functions that have the maximum positive and maximum negative slopes are considered, and the LS estimator is applied on the difference between the corresponding data.

The resulting new estimator will be denoted as LSd2 estimator. The LSd2 estimator is applied using the following steps:

1. Acquire N samples from the four detectors, Equations (4).
2. Compute a prior estimate for the frequency, using the LS estimator in Equation (5).
3. At the prior estimate, determine the two transfer functions that have the maximum positive and the maximum negative slopes. Let these transfer functions be G_m and G_n.
4. Find the LSd2 estimator as the value that minimizes the function $J_d(f)$. Minimization is performed in the neighbourhood of the LS estimate.

$$\begin{aligned} J_d(f) &= \sum_{i=1}^{N} \left[(Z_m[i] - Z_n[i]) - (G_m(f) - G_n(f)) \right]^2 \\ \hat{f}_{0\_\mathrm{LSd2}} &= \min_f \left(J_d(f) \right) \end{aligned} \tag{9}$$

The variance and the maximum bias of the LSd2 estimator are (see Appendix A)

$$\text{var}\left(\hat{f}_{0\_\text{LSd2}}\right) \approx \frac{2\sigma^2/N}{\left(G'_m(f_0) - G'_n(f_0)\right)^2} \tag{10}$$

$$\max\_\text{bias}\left(\hat{f}_{0\_\text{LSd2}}\right) \approx \frac{2e_{\max}}{|G'_m(f_0) - G'_n(f_0)|} \tag{11}$$

It can be proven that the maximum bias of the LSd2 estimator is lower than that of the LS estimator. However, in this paper we will be content with simulation results.

An important issue for an IFM system is the response time. Calculating the LS estimator requires computing the function $J(f)$ and finding its minimum (see Equation (5)), which will need some time to be performed. It is shown in [7] that using a medium density Field Programmable Gate Array (FPGA) as a calculation platform, this task can be performed within 1 µs.

5. DESIGNING THE FREQUENCY RESPONSE OF THE FILTERS

Designing the frequency response of the four filters is an essential step in the design. The frequency response of these filters will determine the accuracy of the IFM system. The selection of the filters type, degree, center frequency, and bandwidth is not limited to those used in this design. Any other selections can be made, if their frequency responses meet the following constraints.

Note that the minimum detectable power for the used detector is $P_{\text{det-min}} = -60\,\text{dBm}$, thus the signal power at the detector input must be higher than $P_{\text{det-min}}$ i.e.,

$$P_{\text{sat}} - 6\,\text{dB} + |S_{21}| > P_{\text{det-min}} \tag{12}$$

where $-6\,\text{dB}$ is the power attenuation caused by the 4-way power divider, and S_{21} is the transmission coefficient of the filter connected to the detector, expressed in dB.

In this design, the output power level P_{sat} for the used limiting amplifier is 0 dBm, thus the usable part of the filter frequency response has an amplitude higher than $-54\,\text{dBm}$.

The filters must be designed so that the usable parts of their frequency responses cover the working frequency band of the system. Also, as mentioned previously, at each frequency point, there must exist one filter with a frequency response that has a significant positive slope, and another filter with a frequency response that has a significant negative slope.

The filters were designed using the design and simulation tools provided by Advanced Design System (ADS) software. The frequency responses of the filters were adjusted to minimize the maximum bias of the estimator. The maximum bias can be computed from Equation (11). This shows the importance of Equation (11), in that it provides a prior knowledge about the accuracy of the resulting estimator, and thus, it can be used to adjust the frequency response of the filters.

Adjusting the frequency response of the filters includes: adjusting the centre frequency, bandwidth, and degree of the filter.

Note that increasing the degree of the filters will increase the time delay for the output signal to reach its steady state, which will increase the response time of the system. In this work, the time delay from the divider input to the filters output is measured using simulation tools in ADS software, and it is less than 25 ns.

6. SIMULATION RESULTS

The performance of the designed IFM system was determined using Monte-Carlo simulation. The data model in Equation (4) and the measured transfer functions shown in Figure 7 were adopted for simulation. The variance and maximum bias of the LSd2 estimator were computed and compared with that of the LS estimator.

The simulation was performed under the following assumptions:

- The noises n_1, n_2, n_3, n_4 are uncorrelated white Gaussian noise voltages with zero mean and variance of $\sigma^2 = (5\,\text{mV})^2$.
- The number of acquired samples is $N = 50$.

- The voltage drifts e_0, e_1, e_2, e_3, e_4 are independent uniform random variables within the interval $-e_{\max}$ to $e_{\max}$ where $e_{\max} = 10\,\text{mV}$, and they were fixed in each simulation run.

Noting that the variation of the output power level P_{sat} of the limiting amplifier and the variation of the detectors output with temperature are stated to be about $\pm 0.4\,\text{dB}$, and this value corresponds to voltage drifts e_0, e_1, e_2, e_3, e_4 of about $\pm 10\,\text{mV}$.

Figure 8(a) shows the standard deviation (STD) of the LSd2 and LS estimators. It is seen that the STD is less than 0.5 MHz for both estimators.

Figure 8(b) shows the maximum absolute bias of the LSd2 and LS estimators. It is seen that the LSd2 estimator has a lower bias than that of the LS estimator, and the improvement attains 25% at some frequencies. The maximum bias is less than 13 MHz for the LS estimator and less than 11 MHz for the LSd2 estimator.

As a conclusion, the LSd2 estimator has a lower bias than that of the LS estimator. This design also shows a maximum bias of about 11 MHz, which is lower than the 15 MHz achieved from the design presented in our previous work.

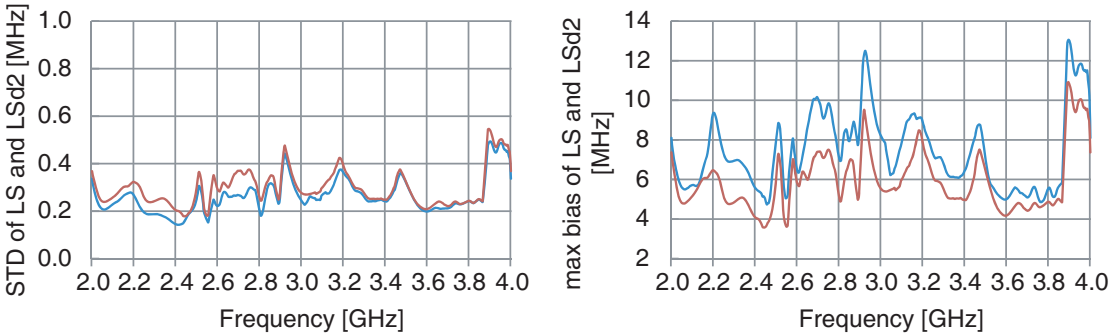

Figure 8. (a) STD of the LSd2 estimator (red), and LS estimator (blue), (b) the maximum bias of the LSd2 estimator (red), and the LS estimator (blue).

7. CONCLUSION

In this paper, a simple design for a 2 to 4 GHz IFM system is presented. The system uses four band-pass filters instead of delay lines to estimate the frequency of the incoming RF signal. A special condition was imposed on the frequency response of the filters, and a new method for estimating the frequency value was proposed. Closed forms for the accuracy of the new estimator were derived and used to adjust the frequency response of the filters. The designed system was implemented and measured at a laboratory. For practical values of noise and measurements error, it showed a maximum error of less than 11 MHz.

APPENDIX A.

The acquired data $Z_1[i], Z_2[i], Z_3[i], Z_4[i]$ in Equation (4) are used to estimate the frequency f_0 of the incoming signal. Assume that the Least Square (LS) estimator (Equation (5)) is used to compute a prior estimate $\hat{f}_{0-\text{LS}}$ for f_0 and that the transfer functions that has the maximum positive and maximum negative slopes, at this prior estimate, are G_m and G_n, respectively. Then the LSd2 estimator ($\hat{f}_{0-\text{LSd2}}$) is calculated as the value that minimizes the function $J_d(f)$. Minimizing of $J_d(f)$ is performed in the neighborhood of $\hat{f}_{0-\text{LS}}$.

$$J_d(f) = \sum_{i=1}^{N} \left[(Z_m[i] - Z_n[i]) - (G_m(f) - G_n(f)) \right]^2 \tag{A1}$$

Minimizing the function $J_d(f)$ is equivalent to solving the equation:

$$\left.\frac{\partial J_d(f)}{\partial f}\right|_{f=\hat{f}_{0-\mathrm{LSd2}}} = 0 = -\sum_{i=1}^{N}\left\{2\left[(Z_m[i]-Z_n[i])-\left(G_m(\hat{f}_{0-\mathrm{LSd2}})-G_n(\hat{f}_{0-\mathrm{LSd2}})\right)\right]\right.$$
$$\left.\left(G'_m(\hat{f}_{0-\mathrm{LSd2}})-G'_n(\hat{f}_{0-\mathrm{LSd2}})\right)\right\} \tag{A2}$$

where $G'(f)$ is the derivative of the transfer function $G(f)$ with respect to frequency.

To simplify the equations, we define the function $D(f)$ as:

$$D(f) \triangleq G_m(f)-G_n(f) \Rightarrow D'(f)=G'_m(f)-G'_n(f) \tag{A3}$$

Replacing $Z_m[i]$ and $Z_n[i]$ from Eq. (4) into Eq. (A2), and using Eq. (A3), gives

$$-\sum_{i=1}^{N} 2\left[D(f_0)+e_m-e_n+n_m[i]-n_n[i]-D(\hat{f}_{0-\mathrm{LSd2}})\right]D'(\hat{f}_{0-\mathrm{LSd2}})=0 \tag{A4}$$

And this leads to solving the equation:

$$\left(D(f_0)+e_m-e_n+\bar{n}_m-\bar{n}_n-D(\hat{f}_{0-\mathrm{LSd2}})\right)D'(\hat{f}_{0-\mathrm{LSd2}})=0 \tag{A5}$$

where:

$$\bar{n}_m=\frac{1}{N}\sum_{i=1}^{N}n_m[i], \quad \bar{n}_n=\frac{1}{N}\sum_{i=1}^{N}n_n[i]$$

Taking into account that the frequency responses of the band-pass filters do not suffer from fast changes, the function $D(f)$ can be approximated by a straight line in the neighborhood of f_0, i.e.,

$$D(f_0)-D(\hat{f}_{0-\mathrm{LSd2}}) \approx (f_0-\hat{f}_{0-\mathrm{LSd2}})D'(f_0) \tag{A6}$$
$$D'(\hat{f}_{0-\mathrm{LSd2}}) \approx D'(f_0) \tag{A7}$$

Replacing Eqs. (A6) and (A7) into Eq. (A5) and rearranging gives

$$\hat{f}_{0-\mathrm{LSd2}}-f_0 \approx \frac{e_m-e_n+\bar{n}_m-\bar{n}_n}{D'(f_0)} \tag{A8}$$

Taking the variance of both sides of Eq. (A8) gives the variance of the LSd2 estimator:

$$\mathrm{var}\left(\hat{f}_{0\_\mathrm{LSd2}}\right) \approx \frac{2\sigma^2/N}{\left(G'_m(f_0)-G'_n(f_0)\right)^2} \tag{A9}$$

Taking the expectation of both sides of Eq. (A8) gives the bias of the LSd2 estimator.

$$\mathrm{bias}(\hat{f}_{0-\mathrm{LSd2}}) \approx \frac{e_m-e_n}{G'_m(f_0)-G'_n(f_0)} \tag{A10}$$

Assuming that the maximum absolute value of the voltage drifts e_m and e_n is $e_{\max}$, the maximum absolute bias of the LSd2 estimator is:

$$\max\_\mathrm{bias}\left(\hat{f}_{0\_\mathrm{LSd2}}\right) \approx \frac{2e_{\max}}{|G'_m(f_0)-G'_n(f_0)|} \tag{A11}$$

REFERENCES

1. East, P. W., "Fifty years of instantaneous frequency measurement," *IET Radar, Sonar & Navigation*, Vol. 6, No. 2, 112–122, 2012.
2. De Oliveira, B. G. M., F. R. L. e Silva, M. T. de Melo, and L. R. G. S. L. Novo, "A new coplanar interferometer for a 5–6 GHz instantaneous frequency measurement system," *IEEE Microwave and Optoelectronics Conference*, Belem, Brazil, Nov. 2009.

3. De Souza, M. F. A., F. R. L. e Silva, and M. T. de Melo, "A novel LSB discriminator for a 5 bit IFM subsystem based on microstrip band-stop filter," *Proc. 38th European Microwave Conf.*, 36–39, Amsterdam, The Netherlands, Oct. 2008.
4. Sandhyarani, S. and T. Kavitha, "Design and implementation of DIFM algorithm in FPGA," *Global Journal of Advanced Engineering Technologies*, Vol. 2, No. 3, 83–88, 2013.
5. Pandolfi, C., E. Fitini, G. Gabrielli, E. Megna, and A. Zaccaron, "Comparison of analog IFM and digital frequency measurement receivers for electronic warfare," *Proc. 7th European Radar Conf.*, 232–235, Paris, France, 2010.
6. De Souza, M. F. A., F. R. L. e Silva, M. T. de Melo, and L. R. G. S. L. Novo, "Discriminator for instantaneous frequency measurement subsystem based on open-loop resonators," *IEEE Trans. on Microwave Theory and Tech.*, Vol. 57, No. 9, 2224–2231, Sep. 2009.
7. Badran, H. and M. Deeb, "A new low cost instantaneous frequency measurement system," *Progress In Electromagnetics Research M*, Vol. 59, 171–180, 2017.